Draft version August 12, 2009
Preprint typeset using LaTeX style emulateapj v. 03/07/07

FOCAL PLANE MASKS FOR ACHROMATIC CORONAGRAPHY

Olivier Guyon
National Astronomical Observatory of Japan, Subaru Telescope, Hilo, HI 96720 and
Steward Observatory, University of Arizona, Tucson, AZ 85721

Frantz Martinache
National Astronomical Observatory of Japan, Subaru Telescope, Hilo, HI 96720

Ruslan Belikov
NASA Ames Research Center
Draft version August 12, 2009

ABSTRACT

Most coronagraph designs require focal plane masks with a given complex amplitude transmission map. A solution to design such masks for polychromatic use in a Lyot configuration (a Lyot mask blocks light outstide the geometric pupil after the focal plane mask) is proposed. This solution relies on the combination of (1) a "smoothing" of the mask edges which does not affect the light within the Lyot mask opening and (2) the addition of sub-λ/D features on the mask; these features diffract light outside the geometrical pupil and alter the transmitted light to achromatize the coronagraph.

Subject headings: instrumentation: adaptive optics — techniques: high angular resolution

1. INTRODUCTION

Direct imaging of exoplanets requires nearly total rejection of light from the central star. Coronagraphs are optical systems designed for this purpose, and many high performance coronagraph concepts have been proposed in the last decade. Most coronagraphs achieve starlight suppression with a focal plane mask, often combined with entrance pupil apodization or/and a Lyot pupil mask. A key requirement for coronagraph systems is the ability to function in a finite spectral band.

While the Lyot mask is naturally achromatic and amplitude apodization of the entrance pupil can be achieved achromatically with either a binary mask (shaped pupil) or a geometric remapping (PIAA), achromatization of the focal plane mask is challenging, and must overcome two issues:

- **Complex amplitude achromaticity:** The phase and/or amplitude transmission of the focal plane mask needs to be achromatic.
- **Size achromaticity:** The focal plane mask physical size should scale linearly with wavelength to maintain a constant size in λ/D unit.

The phase mask coronagraph concept, originally proposed by (**?**) illustrates how these issues can be mitigated at the expense of coronagraph performance and focal plane mask design complexity. In the original concept, the focal plane mask was a $\lambda/2$ phase-shifting circular mask, and both the complex amplitude achromaticity and the size achromaticity were therefore problematic. With mild pupil apodization, the phase mask coronagraph offers total on-axis extinction for any pupil shape and a sub-λ/D inner working angle. **?** showed that both chromaticity issues can be reduced with a dual-zone focal plane mask. The size and phase-shifting properties of each zone were chosen to optimize the coronagraph performance in a sprectral band. Although a significant performance improvement was obtained, their solution could not reach the high contrast required to detect exoplanet from space in a broad spectral band. **?** proposed to use a scale-invariant four-quadrant phase mask to solve the size achromaticity issue, but this new concept however does not offer complete extinction for centrally obscured pupils and the planet light is also extinguisghed when its position falls along the seams between the four quadrants. This last problem is solved in the optical vortex coronagraph (), where the phase is a linear function of the position angle θ around the optical axis. For both the 4 quadrant coronagraph and optical vortex coronagraph, the complex amplitude achromaticity is challenging to solve, especially at high contrast. Achromatic phase shifts may be obtained by stacking carefully chosen thicknesses of materials with different refractive indexes, or with polarization plates.

Several authors have proposed to use chromatic lenses to force the pupil size to be physically inversely proportional to the wavelenght ahead of the coronagraph focal plane mask. This approach, first developped by **?** solves the size chromaticity issue in the coronagraph, and has been successfully used for speckle imaging in broadband light.

Both achromaticity issues are solved if the focal plane mask is fully opaque and large enough to block almost all starlight. This is the approach taken by the shaped pupil coronagraph, which can therefore deliver high contrast simultaneously across a wide spectral band. At high contrast, the coronagraphic performance (throughput and inner working angle) of this scheme is unfortunately significantly lower than for the phase mask coronagraphs described above. A better solution is to perform the pupil apodization by geometrical remapping without loosing light. Using this approach, the Phase-Induced

Electronic address: guyon@naoj.org

Amplitude Apodization (PIAA) coronagraph offers both high coronagraphic performance (high throughput and small inner working angle) and good achromaticity with a fully opaque focal plane mask. Even for the high performance PIAA coronagraph, solving for the chromaticity issues outlined above could however significantly improve the coronagraph's performance:

- The physical size of the focal plane mask has to be set for the red end of the spectral coverage, and the effective inner working angle therefore increases with spectral bandwidth.

- **?** showed that the PIAA coronagraph inner working angle could be further reduced if a partially transmissive phase-shifting focal plane mask is used. With this PIAA complex mask coronagraph (PIAACMC) concept, direct detection of Jupiter analogs in reflected light is possible at 50% throughput at $\approx 1.2\lambda/D$ instead of $1.6\lambda/D$ for a "regular" PIAA coronagraph.

While most previous attempts at achromatizing the focal plane mask have treated the two chromatic issues separately, we propose to simultaneously address both issues by redesigning the focal plane mask. Our approach is somewhat similar to **?**'s dual zone phase mask technique, where additional degrees of freedom are added the phase mask design to better fit the requirement. We however identify a deterministic design technique which can produce a phase mask with the desired complex amplitude as a function of wavelength. Our approach is universal and can be applied to any mask type, regardless of its complex amplitude transmission "2D map", and we show that the masks are manufacturable and the design process can be tuned to take into account a wide range of manufacting limitations. Our approach relies on two core principles: (1) the ability to design, using a single transmissive material, a transmission "cell" with an arbitrary complex amplitude transmission (detailed in §2), and (2) a smoothing of the mask features with no impact on the coronagraph behavior (detailed in §3). We show in §**??** with a few representative examples that these two techniques, when combined, can produce the required phase masks, and that these masks can be manufactured.

2. CHROMATIC CONTROL OF TRANSMITTED PHASE AND AMPLITUDE

2.1. *Semi-periodic array of cells: principle*

The technique proposed in this paper for chromatic control of phase and amplitude is shown in Figure 1. The focal plane mask is made of a single material with a flat surface on one side and a non-flat surface on the other size. The non-flat surface is defined as a semi-periodic array of square "cells". The size of each cell is chosen to be larger than the wavelength λ but smaller than the physical size of the diffraction limit λ/D in the focal plane. The array is semi-periodic because the properties of the cells change accross the mask to obtain complex amplitude multiplication required for the coronagraph to properly function.

We assume in this section that the array is perfectly periodic. The complex transmission of the cell array is

$$T(\lambda) = \int e^{i\frac{2\pi(n(\lambda)-1)f(x,y)}{\lambda}} dxdy \tag{1}$$

where $n(\lambda)$ is the index of refraction of the material used, and $f(x,y)$ is the 3-D surface, or local thickness, of each cell. The coordinates x and y are scaled to the size of each cell (the two opposite corners of a cell are $(x,y)=(0,0)$ and $(x,y)=(1,1)$).

2.2. *Cell design*

Equation 1 shows that the location of the "high" and "low" parts of the 3-D surface within each cell does not affect $T(\lambda)$. The equation can therefore be rewritten as

$$T(\lambda) = \int_{-\infty}^{\infty} h(t)\, e^{i\frac{2\pi(n(\lambda)-1)t}{\lambda}} dt \tag{2}$$

where t is the local thickness of the plate and $h(t)$ is the histogram distribution of the thickess across the cell ($\int_{-\infty}^{\infty} h(t)dt = 1$). This equation can be rewritten as a Fourier transform by using the pseudo wavelength variable $\lambda' = (n(\lambda)-1)/\lambda$:

$$T(\lambda') = \int_{-\infty}^{\infty} h(t) e^{i2\pi t\lambda'} d\lambda' \tag{3}$$

The cell can be therfore be designed by computing the inverse Fourier transform of the transmission function written as a function of λ':

$$h(t) = -\int_{-\infty}^{\infty} T(\lambda') e^{-i2\pi t\lambda'} d\lambda' \tag{4}$$

Equation 4 may not produce a physical solution, as $h(t)$ cannot be negative. An iterative algorithm based upon equation 4 is therefore used to find the solution. The steps necessary to solve for the cell design are :

1. The desired transmission function $T(\lambda)$ is rewritten as $T_0(\lambda')$ with $\lambda' = (n(\lambda)-1)/\lambda$

2. **Initialization:** The transmission function $T(\lambda')$ within the iterative algorithm is initialized to $T_0(\lambda')$.

3. An estimate of $h(t)$ is computed as the inverse Fourier transform of $T(\lambda')$ (equation 4).

4. Negative values of $h(t)$ are replaced by zero.

5. A new transmission function $T_1(\lambda')$ is computed as the Fourier transform of $h(t)$.

6. **Return to step 3:** $T_1(\lambda')$ values are replaced by $T_0(\lambda')$ values in the λ' range where the desired transmission function is specified. The result is written in $T(\lambda')$ and used as the new input for step 3 of the algorithm.

7. After the required number of iterations, $h(t)$ is used as the thickness distribution function for the cell.

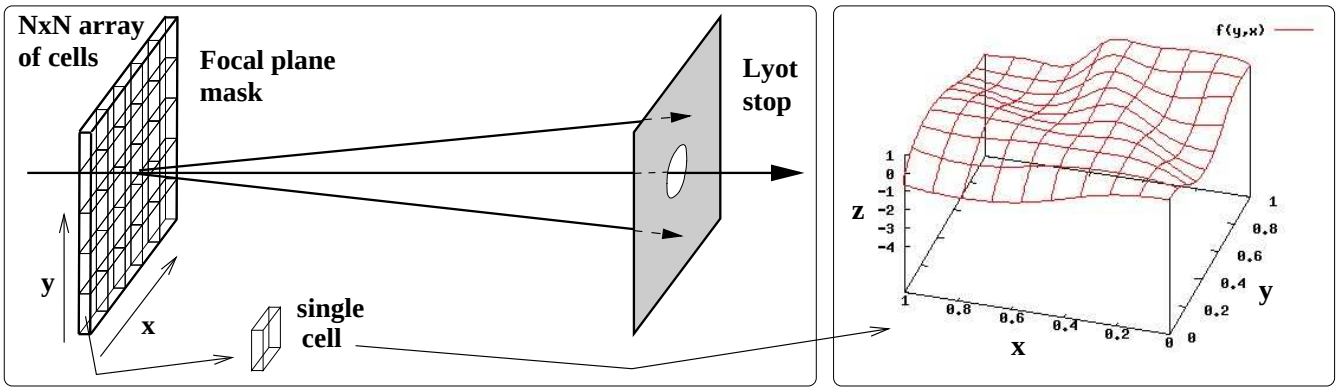

FIG. 1.— Proposed focal plane mask concept. The focal plane mask (left) is made of a quasi-periodic array of cells. The Lyot mask (center) blocks the light diffracted by the array, while light transmitted by the array passes through. Each cell is defined by a 3-D surface designed to produce the required chromatic complex transmission behaviour.

3. FOCAL PLANE MASK "EDGE SMOOTHING"

3.1. *Principle*

The chromatic transmission control scheme discussed in §2 is most efficient when the transmission $T(\lambda)$ varies slowly as a function of λ. A sharp transitions in λ would occur with an "achromatized" hard edged focal plane mask. Such a mask would need to have a constant size in units of λ/D, and its physical edge would therefore move as λ varies. While sharp transitions could be theoretically achieved with the approach discussed in §2, they require precise manufacturing of cells with large thickness variations, and may not be practically manufacturable. Smoothing edges and sharp transitions in the focal plane mask is therefore essential to produce a focal plane mask design which is within manufacturing capabilities. This smoothing is possible because because high spatial frequencies in the focal plane mask diffract light outside of the opening in the Lyot mask: they can be removed with no effect on the coronagraphic performance. This smoothing may be achived by convolution of the "nominal" focal plane mask design by a complex amplitude kernel K.

In this section, u, v and x, y denote the coordinates respectively in pupil and focal planes; r_p denotes the pupil radius. The complex amplitude $\Psi_C(u, v)$ in the coronagraph's exit pupil plane (immediately after the Lyot stop) is

$$\Psi_C = \Psi_A \star \left(\widehat{FPM} \times \widehat{K} \right) \times LM \qquad (5)$$

Where Ψ_A is the entrance pupil complex amplitude, FPM is the focal plane mask "nominal" complex amplitude, K is the kernel by which the focal plane mask complex amplitude is convolved and LM is the Lyot stop multiplicative mask (for most coronagraphs, $LM(u, v)$ is equal to 1 if $\sqrt{u^2 + v^2} < r_p$ and 0 otherwise).

The focal plane mask complex amplitude can therefore be convolved by a smoothing kernel $K(x, y)$ with no effect within the Lyot mask opening if the Fourier transform $\widehat{K}(u, v)$ of the convolution kernel is constant within a radius $2r_p$, where r_p is the pupil radius. The maximal size convolution kernel is therefore the half-scale complex Airy function with a first zero at $0.61\lambda/D$. In this case, $\widehat{K}(r) = 1$ for $r < 2r_p$ and $\widehat{K}(r) = 0$ for $r > 2r_p$.

The ringing in this maximal size convolution kernel however produces transmission values above 1 in some areas of the focal plane mask (on the edge of sharp features), and therefore requires an overall reduction of the focal plane mask transmission to bring this peak value at or below 1 so that the mask can be manufactured. This loss in throughput can be mitigated by apodization of the convolution kernel. For example, the kernel can be chosen as the Fourier transform of a disk surrounded by hypergaussian apodization wings:

$$\widehat{K}(r < 2r_p) = 1 \qquad (6)$$

$$\widehat{K}(r > 2r_p) = exp(-(\alpha \times (r - 2r_p)/2r_p)^{\beta}) \qquad (7)$$

If α is large, K becomes close to the critical half-scale Airy pattern. Small values of α will produce a tighter convolution kernel with less ringing and therefore a higher throughput coronagraph.

3.2. *Smoothed mask examples*

Figure 2 shows "smoothed" focal plane mask designs obtained with the method described in §3.1.

3.2.1. *Optical Vortex Coronagraph (OVC) focal plane mask*

The optical vortex coronagraph (OVC) focal plane mask is nominally fully transparent, and introduces a phase shift $\phi = m\theta$, where θ is the polar angular coordinate and m is the mask topological charge (equal to 2 in this example). The singularity at the center of mask is challenging to manufacture (or even to approximate to a high level of accuracy), and smoothing the mask is expected to reduce manufacturing challenges. Due to OVC symetry properties, convolution of the mask complex amplitude by a circular-symetric kernel preserves the mask phase and only modifies the mask amplitude. Figure 2, left, shows the mask amplitude after convolution with two different kernels. The $\alpha = \infty$ kernel is the largest possible kernel (the half-scale Airy pattern), but produces a strong oscillation in the transmission curve. Since the peak mask transmission has to be at or below 100%, this oscillation forces the mask transmission at large angular separations to be reduced. With $\alpha = 1$ and $\beta = 1$, the kernel is smaller and the "ringing" in the amplitude curve is reduced, therefore improving the focal plane mask transmission at large angular separations.

3.2.2. *PIAA complex mask coronagraph (PIAACMC)) focal plane mask*

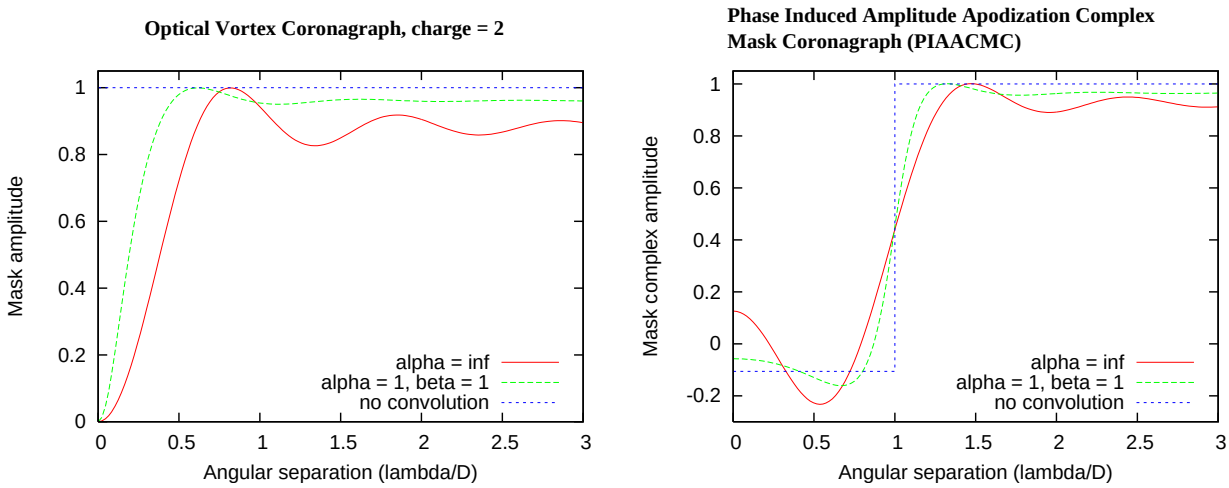

FIG. 2.— Complex amplitude apodization of focal plane masks for the OVC (left) and PIAACMC (right).

The PIAACMC uses a partially transmissive π phase shifting circular focal plane mask. We consider here a $1\lambda/D$ radius mask, which, thanks to the PIAA focal scale magnification effect, offers a $0.90\lambda/D$ inner working angle. The nominal mask complex transmission can be described purely by amplitude, with no phase, and is shown in Figure 2, right: the amplitude transmission is -0.106 within 1 λ/D radius and 1.0 outside the mask. The discontinuity at 1 λ/D is very hard to produce in polychromatic light, as it needs to physically move across the mask as the wavelenght changes. A convolved version of this mask is therefore expected to be significantly easier to manufacture. Figure 2 shows two convolved focal plane mask. The $\alpha = \infty$ solution offers the smoothest mask solution (largest convolution kernel), but the associated ringing reduces the throughput by a few percent at large angular separations. A smaller kernel ($\alpha = 1$, $\beta = 1$) reduces this ringing and improves throughput at large angular separations.

4. CELL DESIGN AND MANUFACTURING

4.1. *Design adopted*

While the transmission properties of the cell are only a function of the thickness distribution across the cell (), the 2D layout adopted for a given thickness distribution has to be carefully chosen to meet manufacturing capabilities.

The design adopted, shown in Figure 3, consists of a stack of discrete rectangular "steps". This design is chosen to be manufactuable by lithography technique, and the steps can be made eithere by material removal of material deposition. To ease manufacturing, the number of discrete material thicknesses should be kept low (less than ≈100) and all cells in the focal plane mask should use the same set of available thicknesses (although different cells will use them in different proportions). The geometry proposed in Figure 3

4.2. *Cell optimization*

5. DISCUSSION

5.1. *Alternative geometries*

Figure 1 shows a square cell geometry, but other geometries can be considered. A circular geometry would be well suited for focal plane masks with a circular symmetry. The focal plane mask would then consist of circular tightly spaced "waves" which would be computed using the algorithm given in §2.

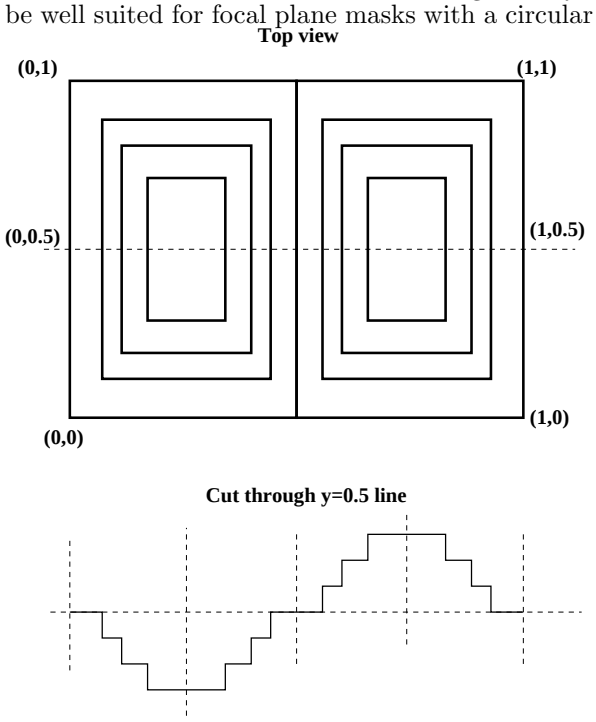

FIG. 3.— Cell design adopted.

5.2. *Amplitude offloading*

5.3. *Manufacturing*

Volume phase holography Diamond turning machining Reflective loss on surface

6. CONCLUSION

REFERENCES

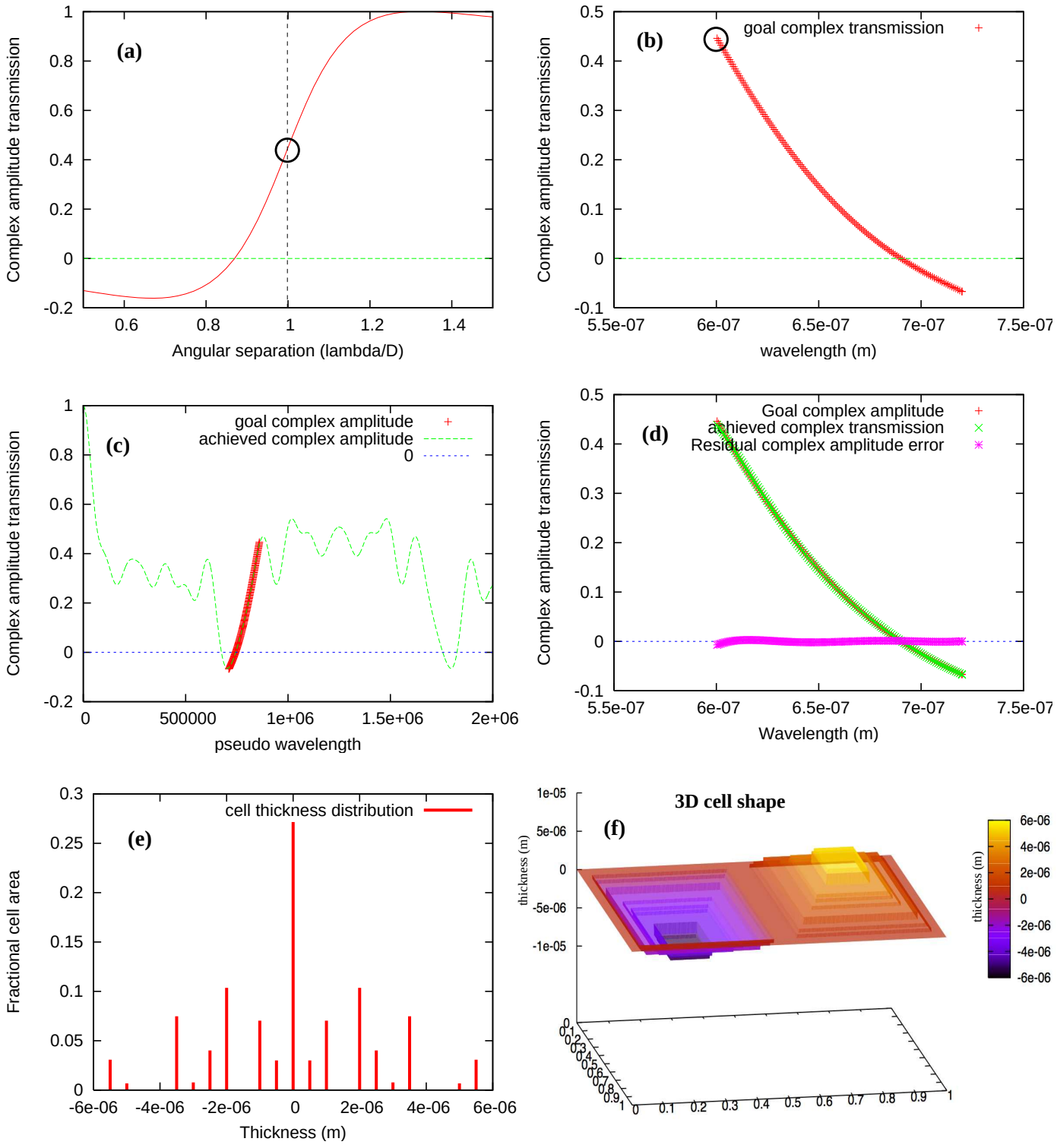

FIG. 4.— Panel (a) shows the PIAACMC's focal plane mask complex amplitude as a function of distance from the optical axis. For a fixed point on the focal plane mask (chosen to be at 1 λ/D for $\lambda = 0.6$ μm), the corresponding complex amplitude as a function of wavelength is shown in panel (b).